Front. Agr. Sci. Eng. 2023, 10(4): 553–565 https://doi.org/10.15302/J-FASE-2023519

RESEARCH ARTICLE

# ENHANCING RAINFALL-RUNOFF POLLUTION MODELING BY INCORPORATION OF NEGLECTED PHYSICAL PROCESSES

Mingjin CHENG[1], Xin LIU[1], Han XIAO[1,2], Fang WANG[2], Minghao PAN[1,2], Zengwei YUAN[1,2], Hu SHENG (✉)[2]

1 State Key Laboratory of Pollution Control and Resource Reuse, School of Environment, Nanjing University, Nanjing 210023, China.

2 Lishui Institute of Ecology and Environment, Nanjing University, Nanjing 211200, China.

**KEYWORDS**

Erhai Lake, field experiment, non-point source, pollution load, rainfall runoff, wash-off model

**HIGHLIGHTS**

- An improved wash-off model integrated with rainfall pollution and SCS-CN is presented.
- Nash-Sutcliffe efficiency coefficients of the enhanced model increased by 2%, 8%, 3% for chemical oxygen demand, total N, total P and 100% for $NH_4^+$-N.
- Two pollution modes dominated by land and rainfall pollutant were identified.
- Refined modeling indicated 12% runoff within 15 min includes 80% to 90% the pollutant load.

Received April 7, 2023;
Accepted August 10, 2023.

Correspondence: shenghu@nju.edu.cn

**GRAPHICAL ABSTRACT**

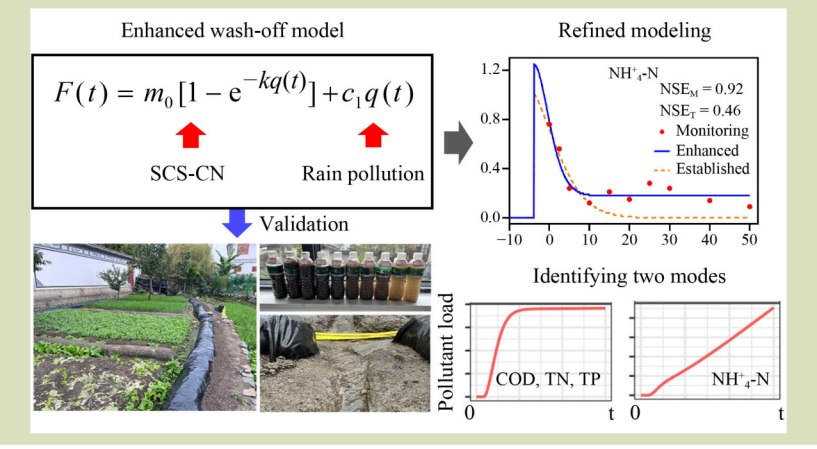


**ABSTRACT**

The growing need to mitigate rainfall-runoff pollution, especially first flush, calls for accurate quantification of pollution load and the refined understanding of its spatial-temporal variation. The wash-off model has advantages in modeling rainfall-runoff pollution due to the inclusion of two key physical processes, build-up and wash-off. However, this disregards pollution load from wet precipitation and the relationship between rainfall and runoff, leading to uncertainties in model outputs. This study integrated the Soil Conservation Service curve number (SCS-CN) into the wash-off model and added pollutant load from wet precipitation to enhance the rainfall-runoff pollution modeling. The enhanced wash-off model was validated in a typical rural-residential area. The results showed that the model performed better than the established wash-off model and the commonly-used event mean concentrations method, and identified two different modes of pollution characteristics dominated by land pollution and rainfall pollution, respectively. In addition, the model simulated more accurate pollutant concentrations at high-temporal-resolution. From this, it was found that 12% of the total runoff contained 80% to 95% of the total load for chemical oxygen demand, total N,

and total P, whereas it contained only 15% of the total load for $NH_4^+$-N. The enhanced model can provide deeper insights into non-point pollution mitigation.



## 1 INTRODUCTION

Rainfall-runoff pollution has been identified as a main contributor to water quality reduction[1–4]. Cost-effective pollution mitigation calls for accurate estimation of pollution load. Although rainfall-runoff monitoring can quantify pollution load in a rain event[5], estimating rainfall-runoff pollution load at larger scales is challenging due to its high spatial-temporal variability[6–8], resulting mainly from various surface conditions and rainfall characteristics[9,10]. Therefore, refined modeling of rainfall-runoff pollution is crucial for estimating pollution load with significant spatial-temporal heterogeneity.

The wash-off model and the event mean concentration (EMC) method have been widely used to quantify rainfall-runoff pollution load and depict the spatial-temporal variation[10,11]. The EMC method simplifies rainfall-runoff process by using mean pollutant concentrations of rain events regardless of physical processes. This deficiency may cause insufficient understanding of spatial-temporal characteristics of runoff pollution, which cannot provide effective information on precision mitigation of first flush, namely the initial stage of a rain event where most of the pollution load is flushed out[12]. Also, surface conditions, especially the pollution accumulation statuses of the same land-use type, are insufficiently considered in the EMC method. To address these deficiencies, the wash-off model, which includes semi-empirical buildup and wash-off routines[13,14], was developed and has been widely used to model the wash-off process of pollutants[15–18]. Initial pollution load which could be washed and rainfall intensity are the two key physical variables in the wash-off model, making important contributions to the uncertainty of model outputs[19]. However, pollution load from wet precipitation is excluded from the model because of the hypothesis that the initial load is pollutant accumulation on dry days. For instance, nitrogen deposition has been regarded as an important pollution source in some regions[20]. In the established wash-off model, the relationship between rainfall intensity and runoff amount is assumed to be linear, which does not consider the time-lag effect when rain stops but runoff still exists[21]. Some physical and machine-learning models, such as Soil Conservation Service curve number (SCS-CN), have been developed to quantify this relationship[22]. The exclusion of these two physical processes hinders fineness improvement of the wash-off model, which may cause large uncertainties in pollution load estimation at high spatial-temporal resolution. This knowledge gap weakens cost-effective mitigation of non-point source pollution.

In previous studies, wash-off models were mainly used in urban areas rather than rural-residential areas because of the perceived lower rainfall-runoff pollution in rural settlement lands due to the smaller share of impervious surfaces[23]. Nevertheless, the landscape of rural-residential areas has significantly changed with the increasing urbanization in recent decades, resulting in incremental impervious surface, growing amounts of wastewater and domestic solid waste, and incomplete waste collection and treatment facilities. This transition has dramatically enlarged the rainfall-runoff pollution in rural areas[5], especially in developing countries with high rural populations. Four surfaces, including roofs, roads, courtyards and vegetable fields, have been commonly selected to monitor and simulate runoff pollution in rural-residential areas[24]. Of these surfaces, vegetable fields have a comparatively heavy pollution load, although the specific characteristics of the resulting runoff pollution remain unclear. Therefore, precise modeling of runoff pollution in vegetable fields assumes importance in comprehending the contribution of rural non-point sources to water pollution and gaining profound insights into effective mitigation strategies.

This paper presents an enhanced wash-off model to improve rainfall-runoff pollution modeling by introducing the pollution load from wet precipitations and using SCS-CN curves to establish the relationships between rainfall intensity and runoff amount. We built an experimental site and tested the enhanced wash-off model by monitoring pollutant concentrations in runoff during a 1 h rain event, in a typical rural-residential area (Gusheng Village) in the Erhai Lake Basin, Yunnan Province, China. The improvements of the enhanced model and the implications for rainfall-runoff pollution management are discussed.

# 2 METHODS

## 2.1 Conceptual model of the rainfall-runoff process

To quantify the rainfall-runoff pollution load, including four typical pollutants of chemical oxygen demand (COD), ammonia nitrogen ($NH_4^+$-N), total nitrogen (TN), and total phosphorus (TP), we present the conceptual model of rainfall-runoff process shown in Fig. 1. A represents the area of a square that is enclosed horizontally with only one outlet and $M(t)$ represents the total amount of pollutants remaining in a rain event at time $t$. Accordingly, the amount of pollution load remained per unit area $m(t)$ can be calculated by $M(t)/A$. Similarly, $Q(t)$ represents the total water flow yield at time $t$, then the runoff depth, $q(t)$, can be calculated by $Q(t)/A$. The runoff intensity, $r(t)$, can also be calculated by $\mathrm{d}q(t)/\mathrm{d}t$. Therefore, the cumulative rainfall-runoff pollution load, $F(t)$, can be calculated by $m(0)-m(t) = m_0-m(t)$. Here, $m_0$ represents the initial pollution load, which can be washed, and is regarded as a part of the surplus after the input and output of pollution load (e.g., fertilizer inputs, crop harvests, leaching and dry precipitation) in the plot (field) during dry days. The instantaneous rainfall-runoff pollution load $f(t)$ can be calculated by $\mathrm{d}F(t)/\mathrm{d}t = -\mathrm{d}m(t)/\mathrm{d}t$. If it is assumed that $f(t)$ is proportional to $r(t)$ and $m(t)$, and the proportionality constant is $k$ which represents wash-off coefficient, the equation of these variables is as follows:

$$f(t) = -\frac{\mathrm{d}m(t)}{\mathrm{d}t} = kr(t)m(t) = k\frac{\mathrm{d}q(t)}{\mathrm{d}t}m(t) \tag{1}$$

Based on Eq. (1), the basic equation for estimating rainfall-runoff pollution load is Eq. (2), and the analytic solution is Eq. (3). When $m(t) = m_0/2$, $q(t) = \ln(2)/k$, which is the runoff of the half-decay of the runoff pollution load in the plot. Also, the cumulative pollution load at time t can be calculated by Eq. (4), and the concentration of pollutants at time t can be calculated by Eq. (5). $c_0 = km_0$ is the initial concentration of pollutants.

$$\frac{\mathrm{d}m(t)}{\mathrm{d}q(t)} = -km(t) \tag{2}$$

$$m(t) = m_0\mathrm{e}^{-kq(t)} \tag{3}$$

$$F(t) = m_0\left[1-\mathrm{e}^{-kq(t)}\right] \tag{4}$$

$$c_{\mathrm{original}}(t) = \frac{f(t)}{r(t)} = km(t) = c_0\mathrm{e}^{-kq(t)} \tag{5}$$

$$\mathrm{EMC}(T) = \frac{F(T)}{q(T)} = \frac{m_0}{q(T)}\left[1-\mathrm{e}^{-kq(T)}\right] \tag{6}$$

The EMCs can be calculated using Eq. (6), where, $T$ is the rainfall-runoff duration.

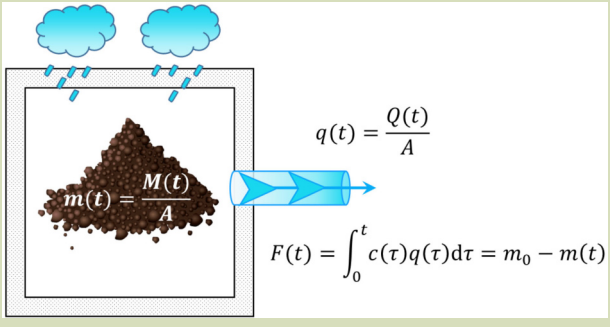


**Fig. 1** Conceptual model for estimating rainfall-runoff pollution load.

## 2.2 Enhanced wash-off model

We enhanced the established wash-off models which was developed by Sartor and Boyd[13]. An implicit assumption of the established wash-off model is that the rain is pure water without any pollutants. Therefore, the concentration of pollutants $c_{\mathrm{original}}(t)$ will tend to zero when the time is long enough (i.e., $t\to\infty$). In fact, when considering the pollutants in the rainfall (i.e., wet precipitation), $c_{\mathrm{original}}(t)$ cannot be zero. Assuming the pollutant concentration of wet precipitation is constant $c_1$, the concentration equation can be modified as Eq. (7). Accordingly, $F(t)$ can be calculated by Eq. (8). The remaining pollution load on the plot is still calculated by Eq. (3).

$$c(t) = c_0\mathrm{e}^{-kq(t)} + c_1 \tag{7}$$

$$F(t) = \int_0^t c(\tau)r(\tau)\mathrm{d}\tau = m_0\left[1-\mathrm{e}^{-kq(t)}\right] + c_1q(t) \tag{8}$$

$$\mathrm{EMC}(T) = \frac{F(T)}{q(T)} = \frac{m_0}{q(T)}\left[1-\mathrm{e}^{-kq(T)}\right] + c_1 \tag{9}$$

Based on this, $F(t)$ can be separated into two parts $F_1(t)$ and $F_2(t)$ to compare which is the leading source of pollution load contribution; where, $F_1(t) = m_0\left[1-\mathrm{e}^{-kq(t)}\right]$ is the cumulative pollution load from the plot at time t, and $F_2(t) = c_1q(t)$ is the cumulative pollution load from the rainfall at time $t$. Additionally, EMCs can be estimated by Eq. (9), and a constant $c_1$ has been added to the original expression. It suggests that the EMC($T$) will be closer to the background concentration of wet precipitation $c_1$ when $T$ becomes longer.

## 2.3 Experimental site description

This study selected a typical rural-residential area located in Gusheng Village within Erhai Lake Basin as the observation

and experimental site to validate the enhanced wash-off model (Fig. 2(a)). Erhai Lake is the second-largest lake in Yunnan-Guizhou Plateau in China, which has an average depth of about 10.5 m and a maximum depth of approximately 21 m. Non-point source pollution and water quality deterioration resulting from rapid socioeconomic development in Erhai Lake Basin have attracted significant attention from the government and the public. To observe the rainfall-runoff process and monitor the pollutant concentration during a rain event, a private courtyard vegetable field was converted into the experimental field by building drainage paths, covering the waterproof membrane and leveling.

To be specific, we first used a drone to capture aerial photos of the selected vegetable field and mapped its boundary. The field area is approximately 135 $m^2$ (Fig. 2(b, c)). Then, we designed the drainage path, dug trenches and built ridges in accordance with the path. The field was divided into four small areas, each of which drains into a single outlet via a drainage ditch (Fig. 2(d)). Next, we enclosed the field with a layer of waterproof membrane to create a closed experimental area that would prevent water from flowing out from areas other than the outlet (Fig. 2(e)). Finally, we leveled the field so that the owner could plant vegetables as usual (Fig. 2(f)).

## 2.4 Data observation and parameter estimation

Based on the experimental field, we observed the runoff during rainfall and collected water samples to monitor water quality indicators, COD, $NH_4^+$-N, TN and TP, within 1 h after the flow generation. Water samples were taken every 5 min in the first 30 min, and then were taken every 10 min in the second

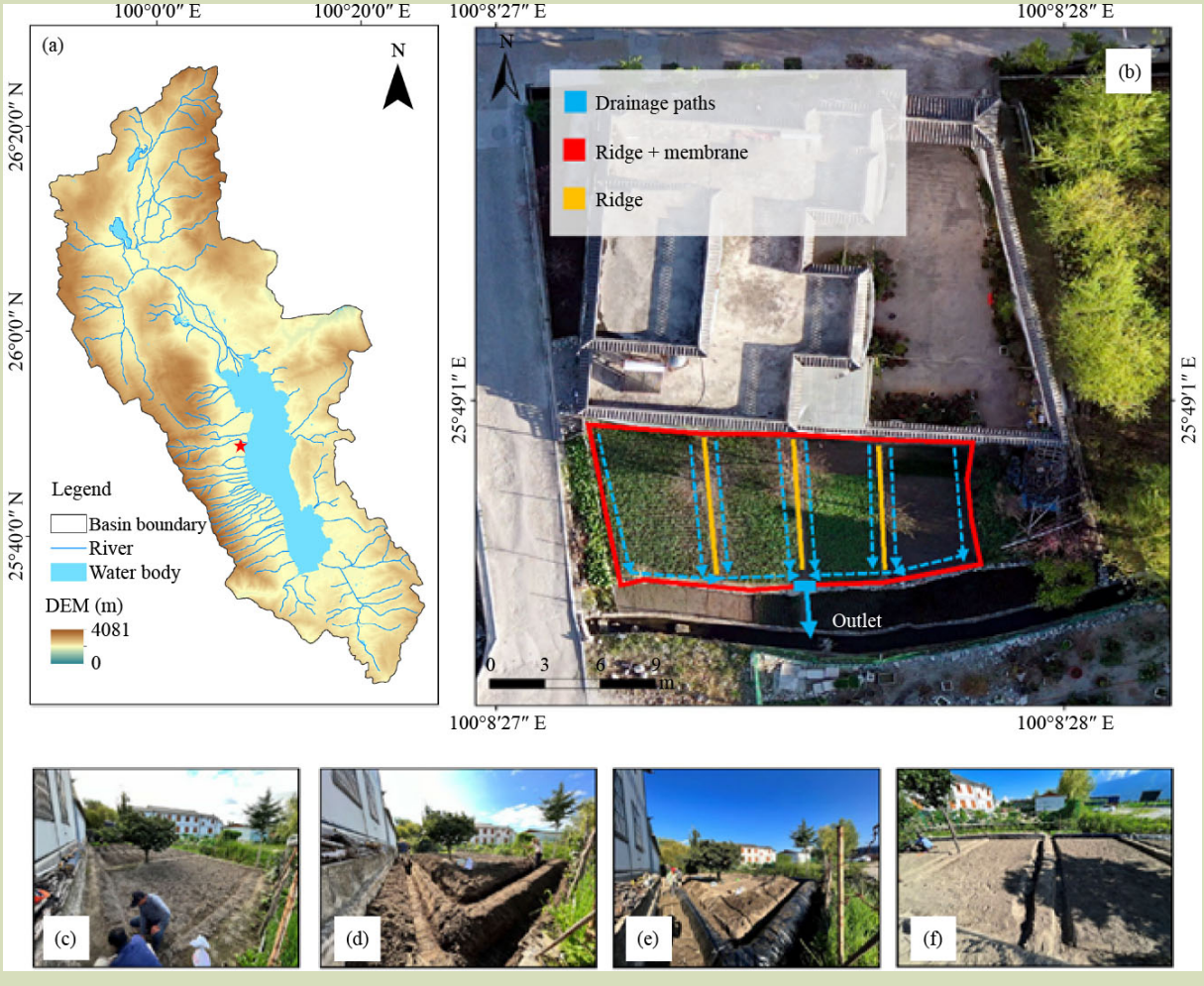


**Fig. 2** Experimental site (审图号: GS 京 (2023) 2266 号). (a) Geolocation of Gusheng village. (b) Experimental vegetable field. (c) Unconstructed field. (d–f) Construction steps including building drainage paths, covering the waterproof membrane and leveling.

30 min. To be specific, we collected and monitored samples from the outlet at 10 time intervals: 0, 2, 5, 10, 15, 20, 25, 30, 40 and 50 min. We used smaller time intervals in the early observation period and larger time intervals in the later period, as the pollutant concentration decays faster in the early period and slower later, according to the model expression. Therefore, more frequent observations during the early period can effectively capture the changes in concentration. Then, we can get the observation sequence of the concentration of the $i$-th pollutant over time: $c^*_{i,t_0}, c^*_{i,t_1}, \cdots, c^*_{i,t_n}$. Theoretically, these concentrations should be obtained with Eq. (10). In principle, $t_0 = 0$, but this was not the case during experiments. Generally, the flow yield occurred before we took the first water sample, because the initial flow was too small to collect. We could only start sampling when the flow became large enough and ignored the time taken by the sampling process. Therefore, the time passed $t_0$ when we took the first sample, and Eq. (10) was modified as Eq. (11).

$$c_i(t) = c_{i,0}\mathrm{e}^{-k_i q(t)} + c_{i,1} \tag{10}$$

$$c_i(t) = c_{i,0}\mathrm{e}^{-k_i q(t+t_0)} + c_{i,1} \tag{11}$$

An unknown function shown in Eq. (11) as $q(t)$ is the runoff depth. Here we couple the SCS-CN method to calculate $q(t)$ using $p(t)$.

$$q(t) = \begin{cases} \dfrac{[p(t)-i_a]^2}{p(t)+S-i_a} = \dfrac{[p(t)-i_a]^2}{p(t)+4i_a}, & p(t) \geqslant i_a \\ 0, & p(t) < i_a \end{cases} \tag{12}$$

where, $p(t)$ is the amount of rainfall, $i_a = \lambda S$, $S$ is the maximum possible infiltration of the soil and $i_a$ is the initial loss. The initial loss $i_a$ is affected by land use, farming methods, irrigation conditions, branch and leaf retention, infiltration, filling and other factors, it has a certain positive relationship with the maximum possible infiltration of the soil $S$, the proportional constant is $\lambda$ (usually 0.2), the initial loss $i_a$ can be obtained by monitoring the rainfall before the production flow and can also be calculated by the relationship with $S$. The SCS-CN method proposes a runoff curve number (i.e., CN) as a composite parameter reflecting the characteristics of the watershed before rainfall to estimate the maximum possible soil infiltration $S$. The larger CN and the smaller $S$, the more likely for runoff to be generated. The main factors determining CN are soil moisture, soil type, vegetation cover type, management status and hydrological conditions. Slope also has some influence on CN. The conversion relationship between $S$ and CN is $S = 25400/\mathrm{CN}-254$.

When the rainfall intensity is constant $i_0$, namely $p(t) = i_0 t$, $q(t)$ can be calculated by Eq. (13) according to the SCS-CN method. Considering the time lag $t_0$, the pollutant concentration can be calculated as Eq. (14).

$$q(t) = \begin{cases} \dfrac{(i_0 t - i_a)^2}{i_0 t + 4i_a}, & i_0 t \geqslant i_a \\ 0, & i_0 t < i_a \end{cases} \tag{13}$$

$$c_i(t) = \begin{cases} c_{i,0}\exp\left\{-k_i \dfrac{[i_0(t+t_0)-i_a]^2}{i_0(t+t_0)+4i_a}\right\} + c_{i,1}, & i_0(t+t_0) > i_a \\ 0, & i_0(t+t_0) \leqslant i_a \end{cases} \tag{14}$$

To estimate the parameters $c_{i,0}$, $k_i$, $t_0$ and $i_a$ ($i_0$ is the observed rain intensity), the Nash-Sutcliffe efficiency coefficient (NSE) was used as the evaluation function of the goodness-of-fit (Eq. (15)). We used the average NSE as the objective function to fit simulated values to observed values (Eq. (16)).

$$\mathrm{NSE}_i = 1 - \frac{\sum_{t=0}^{n}\left(c^*_{i,t} - c_{i,t}\right)^2}{\sum_{t=0}^{n}\left(c^*_{i,t} - \bar{c}^*_{i,t}\right)^2} \tag{15}$$

$$\overline{\mathrm{NSE}} = \frac{1}{N}\sum_{i=1}^{N}\mathrm{NSE}_i \tag{16}$$

where, $\mathrm{NSE}_i$ is NSE of pollutant $i$, $c^*_{i,t}$ is the observed concentration of pollutant i at the time t, $c_{i,t}$ is the simulated concentration of pollutant $i$ at the time $t$, $\bar{c}^*_{i,t}$ is the averaged observed concentration of pollutant i from $t = 0$ to $t = n$, $\overline{\mathrm{NSE}}$ is average NSE of all pollutants and $N$ is the number of pollutants.

# 3 RESULTS

## 3.1 Rainfall-runoff pollution characteristics

Statistical analysis of the four main pollutant indicators during the rain event is presented in Table 1. The coefficient of variation (CV) for all indicators, except $NH_4^+$-N, is greater than 1, indicating significant variation in pollutant indicators during the rain event. In reference to the third-class water quality standard for surface water in China (viz., Environmental quality standards for surface water, GB 3838-2002)[25], the average COD is 51 times greater than the standard, and the maximum 180 times greater. Although both the average and the maximum of $NH_4^+$-N were within the acceptable limits, the average TN is 35 times greater than the standard and the maximum 197 times greater. Similarly, the average TP is 138 times greater than the standard and the maximum 532 times greater. It is evident, therefore, that in addition to NH4$^+$-N, the levels of pollution for the remaining indicators are exceptionally high, particularly for TP.

Table 1 Summary of observed water quality of runoff (mg·L$^{-1}$)

| Indicators | Mean | SD | CV | Max | Min |
|---|---|---|---|---|---|
| COD | 1041.70 | 1174.73 | 1.13 | 3610.00 | 163.00 |
| $NH_4^+$-N | 0.28 | 0.21 | 0.77 | 0.76 | 0.09 |
| TN | 36.27 | 60.42 | 1.67 | 198.00 | 2.40 |
| TP | 27.74 | 34.73 | 1.25 | 106.57 | 3.47 |

We also conducted a correlation analysis on these indicators to investigate the potential synergistic effect among them. Given the high variability of the indicators and to minimize the impact of a few outliers on the correlation analysis, we log-transformed the indicators. As evident in Fig. 3, there is significant correlations between all indicators except for $NH_4^+$-N. The correlation among the other indicators is particularly strong, as indicated by their regression lines and confidence bands (Fig. 3). By combining the univariate analysis and correlation analysis of the four pollutant indicators, we tentatively conclude that there are two modes of pollutant indicators: one is characterized by COD, TN and TP, and the other by $NH_4^+$-N. This is because wet precipitation dominates the $NH_4^+$-N concentration in runoff whereas initial pollution in the plot is leading in other indicators.

## 3.2 Model fitting and validation

We fitted four models to simulate these water quality indicators are shown in Fig. 4 including observed data and simulation curves from enhanced and established models. All NSE values shown exceed 0.9, indicating that the models

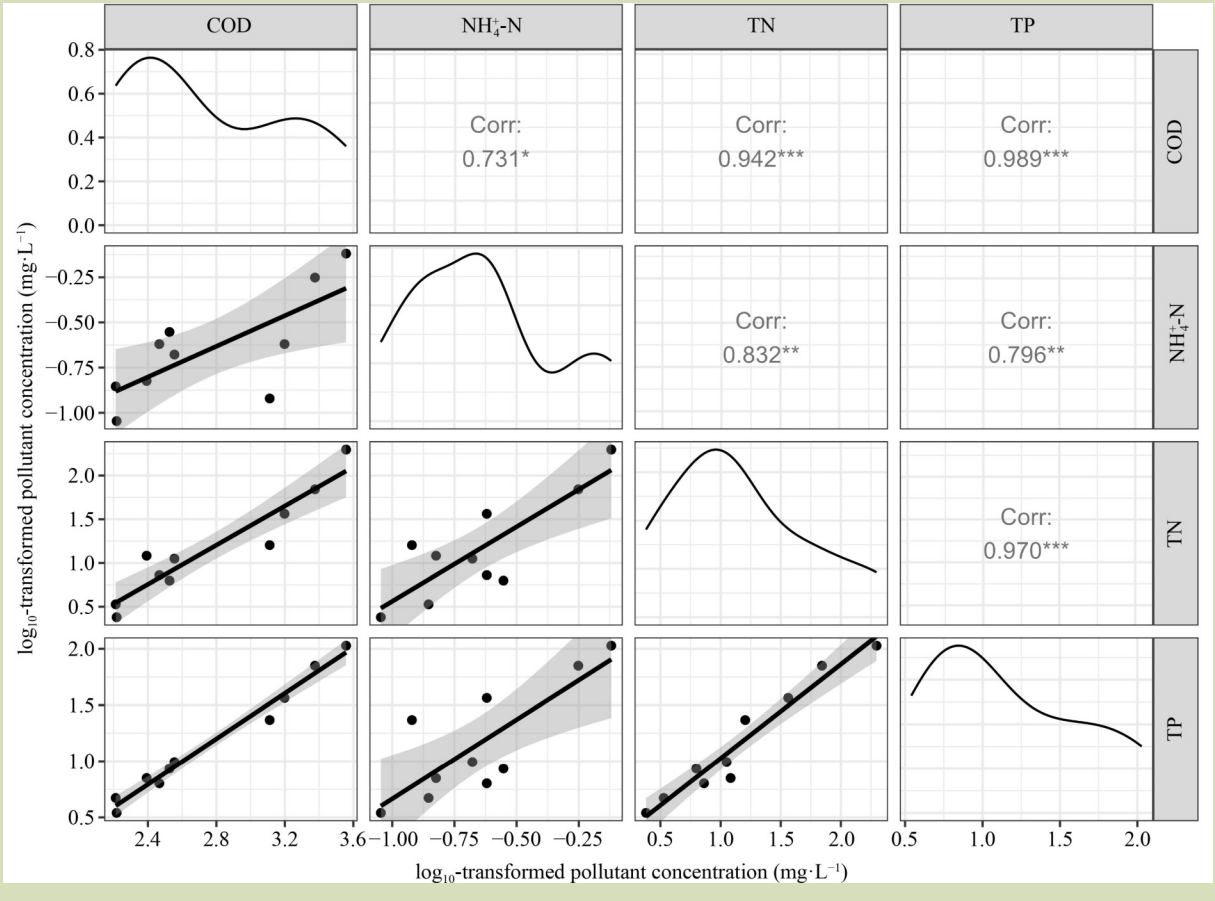


Fig. 3 Correlation analysis of the logarithm of water quality indicators. Gray shading represents the 95% confidence bands.

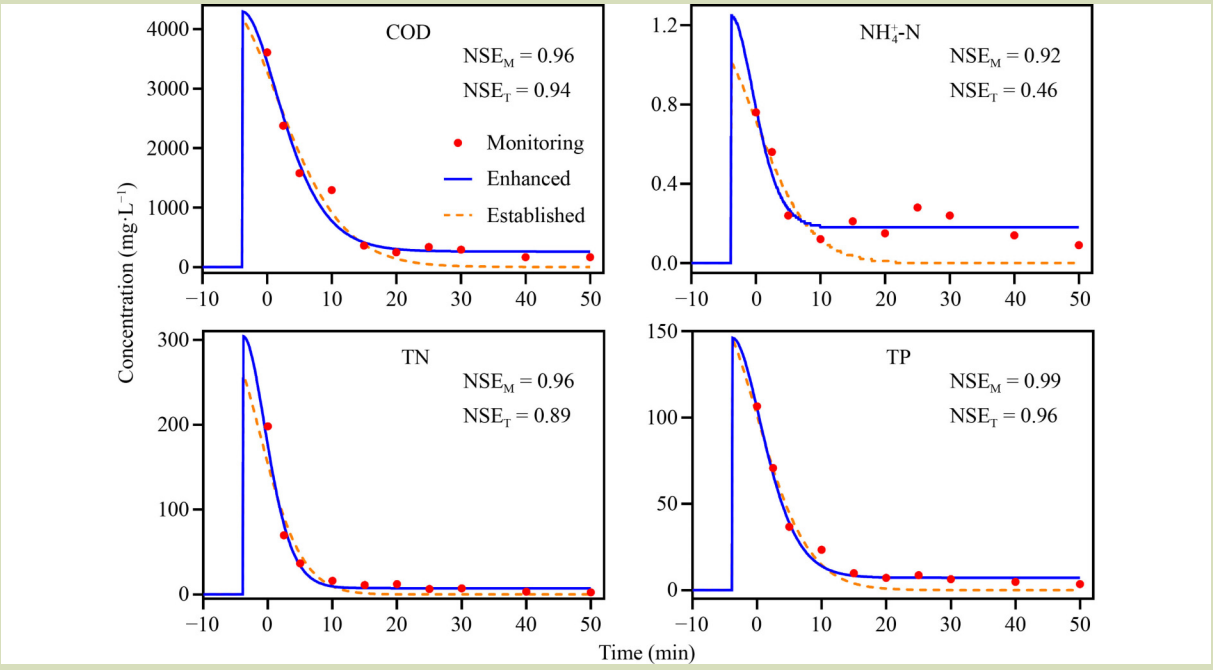


**Fig. 4** Fitting model with observation water quality data. The red dots represent monitoring data. The blue and orange curves represent simulated results from the enhanced and established wash-off models, respectively. $NSE_M$ and $NSE_T$ mean Nash-Sutcliffe efficiency coefficients of the enhanced and established wash-off models, respectively.

perform well in accuracy, especially for TP. Compared with established wash-off model without wet precipitation, the NSE values increase by 2.1%, 100%. 7.9%, and 3.1% for COD, $NH_4^+$-N, TN and TP, respectively. The obvious improvement of $NH_4^+$-N in NSE results from the great contribution of wet precipitation to pollutant concentration of runoff (Fig. 3 and Fig. 5). Additionally, the fitted curves exhibit two noteworthy features: (1) the starting point on the time axis is not zero, which is due to manual implementation of the entire observation process, making it challenging to collect water samples at the exact runoff moment when the water volume is small; and (2) the curve is a horizontal line for a duration of time at the outset, with an intercept of zero, mainly because the runoff event has not been triggered at that point, and the duration corresponds precisely to the time between rainfall and runoff.

Based on the parameter estimation obtained from model fitting, we can generate curves that display the variation of pollutant load with rainfall time for four water quality indicators (Fig. 5). The pollutant load is partitioned into two segments, where $F(t)$ denotes the total pollutant load, $F_1(t)$ signifies the pollutant load from surface runoff, and $F_2(t)$ represents the pollutant load from rainwater itself. Notably, $F_1(t)$ has an S-shaped curve whereas $F_2(t)$ follows an increasing function curve. Also, the shapes of these two curves remain consistent for different water quality indicators. The combination of these curves, $F(t)$, has two clear features. The first is the S-shaped curve for COD, TN and TP and the other is an almost straight-line for $NH_4^+$-N. This result indicates that land sources mainly contribute to COD, TN and TP whereas $NH_4^+$-N primarily originates from atmospheric wet deposition, which precisely explains the discrepancies identified in the characteristic feature of $NH_4^+$-N and other water quality indicators examined earlier (Fig. 3).

### 3.3 More refined modeling by the enhanced model

To show the advances of considering physical processes in runoff modeling, we compared the pollution concentration of runoff using the enhanced wash-off model $c(t)$ and EMC method (Eq. (9)). The changes in EMC are calculated with respect to rainfall duration $T$ (0.1 min) (Fig. 6). Overall, EMC($T$) and $c(t)$ exhibit a similar pattern, with the decay process of EMC($T$) lagging behind that of $c(t)$. After a prolonged rainfall duration, EMC($T$) gradually approaches $c(t)$ whereas $c(t)$ tends toward the concentration of wet deposition $c_1$. It is noteworthy that if the rainfall duration is long enough,

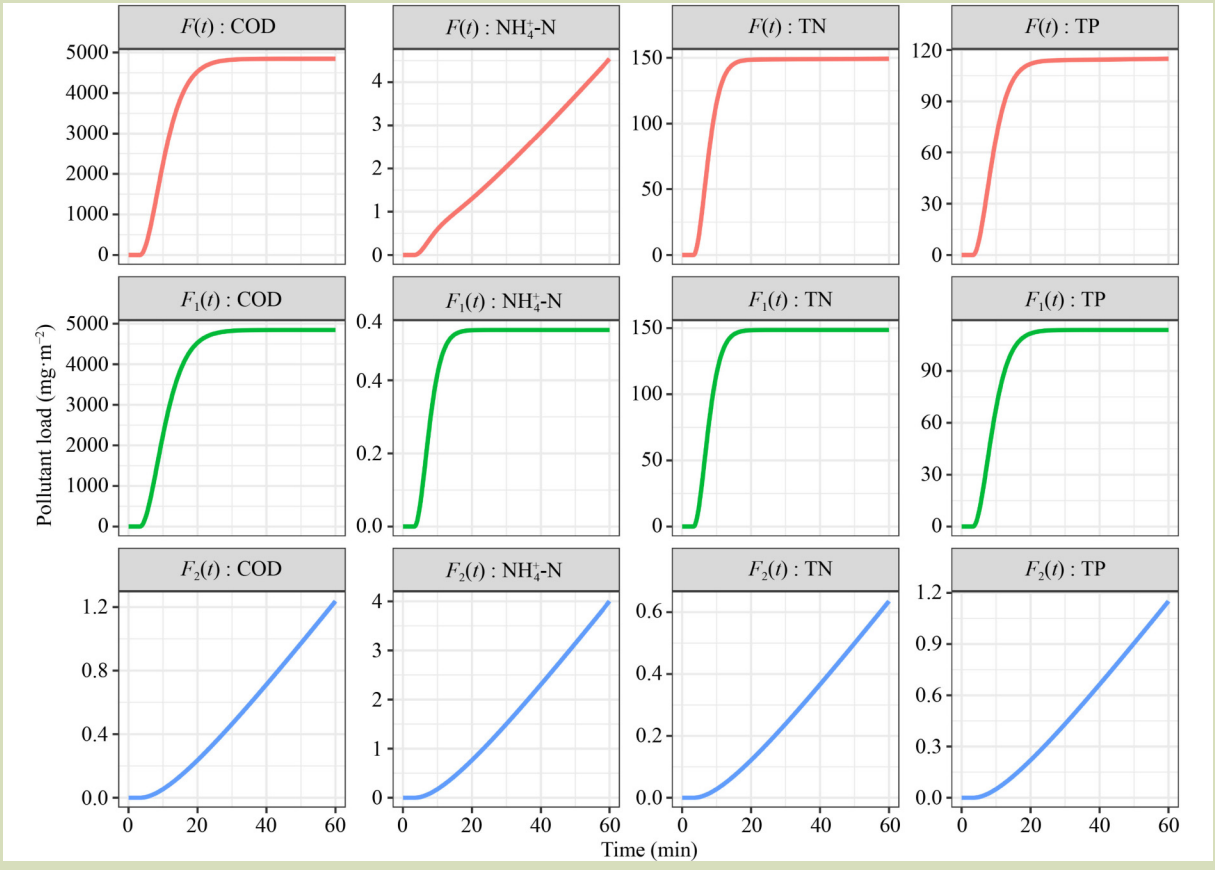


**Fig. 5** Modeling the cumulative rainfall pollutant load $F(t)$. $F_1(t)$ and $F_2(t)$ represent pollution load from surface and wet precipitation, respectively.

EMC($T$) remains relatively stable. However, this condition cannot always be met, especially given the increasing rainfall variability resulting from climate change[26]. Therefore, it is not appropriate to use a constant EMC to characterize the pollutant load washed out by each rain event at a small timescale.

By more accurately modeling temporal variation, we investigated the influence of model improvement on the time duration estimation of first flush. Assuming this rainfall lasted for an hour, we calculated the relationship between changes in water volume and pollution load during different time intervals within the hour. The results are presented in Fig. 7. These data shows that within the first 15 min, about 12% of the runoff carries roughly 80% of the COD load, 95% of the TN load and 90% of the TP load. This indicates that intercepting only 12% of the runoff in the first 15 min can significantly reduce these pollution loads. This finding is beneficial for implementing control measures aimed at mitigating non-point source pollution in rural-residential areas.

# 4 DISCUSSION

## 4.1 Improvements of the enhanced model

Established wash-off models were developed to quantify contaminants, especially particulates containing heavy metals from road/street/highway to water bodies by wash-off[9,11,13,27,28]. Although established wash-off models have been improved over time[14,15,29–31], the role of wet precipitation has been largely ignored. In addition, earlier research also overlooked the indirect inputs of atmospheric deposition to water bodies through runoff, focusing solely on direct precipitation[32,33]. However, this study found that introducing wet precipitation can both enhance the accuracy of wash-off model (Fig. 4) and reveal distinct characteristics of pollutants. The introduction of wet precipitation expands the two processes (build-up and wash-off) into three, thus improving the physical mechanism of wash-off model and addressing the problem of zero pollution load in runoff during the later stage of a rain event. This improvement should be significant in regions with polluted rainfall. The enhanced

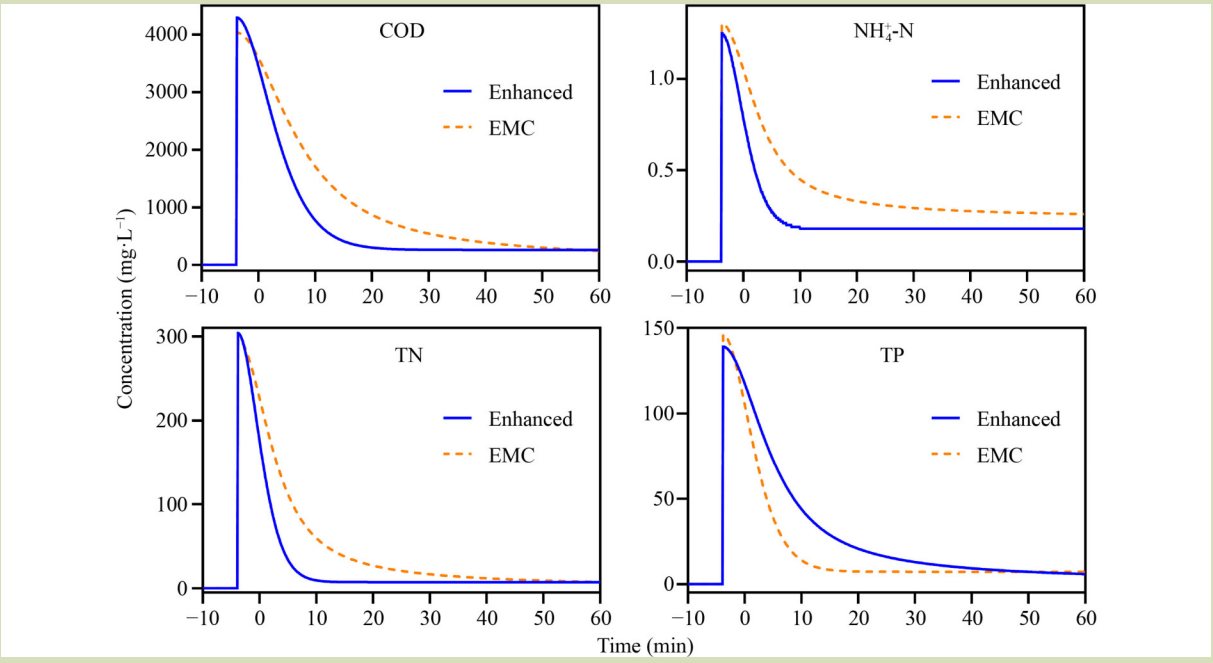


**Fig. 6** Comparison of simulated pollutant concentration in runoff between the enhanced wash-off model and EMC method.

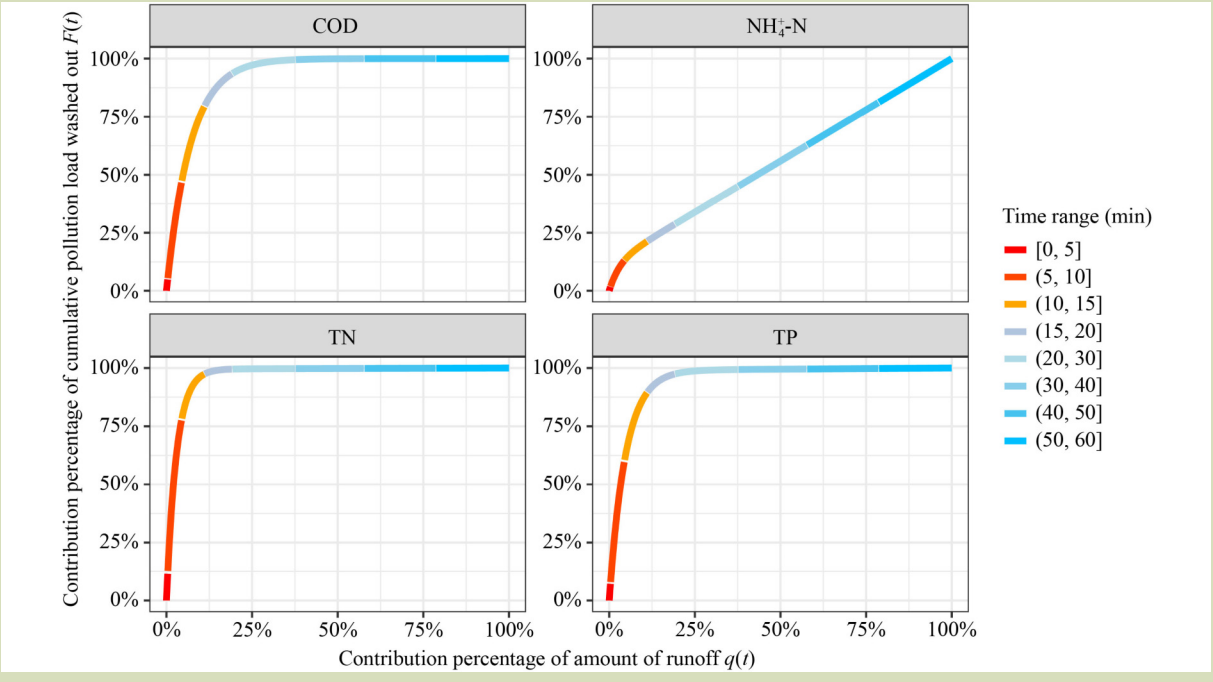


**Fig. 7** Comparing the contributions of runoff $q(t)$ and cumulative pollution load washed out $F(t)$ at various time ranges.

model can differentiate two modes, the S-shaped curve dominated by land pollution and the straight-line curve dominated by wet precipitation (Fig. 5). Consequently, different control measures are required for different pollutants. In addition to wet precipitation, SCS-CN method estimates runoff yield based on the amount of rainfall and underlying

surface. Accordingly, the pollution load simulated by the enhanced model shows a delay effect compared to established wash-off models using rainfall as $q(t)$. This improvement enables researchers to consider the influence of rainfall characteristics including intensity and interval between rainfall events.

The wash-off model simulates the generation of pollutants in runoff, which is the back end of pollution accumulation and the front-end of migration and transformation of pollutants. Compared to EMC method, the enhanced model provides data interfaces for researchers. As Eq. (8) shows, $m_0$ is part of the surplus pollutant load, which can be calculated by nutrient budget[34,35] or material/substance flow analysis[33,36]. In these studies, environmental costs are typically presented as material losses (i.e., input minus output), regardless of the difference between pollution generation and emission. Parameter $k$ represents the difficulty of pollutants to wash out by runoff and accounts for factors such as land types, slopes, soil types and vegetation. Parameters $m_0$ and $k$ enable the depiction of the spatial heterogeneity of rainfall-runoff pollution using high-resolution information on human activities[37–40], instead of monitoring and calculating EMCs in many regions. As evident in Fig. 6, compared to the EMC method, which tends to overestimate pollutant concentrations during most stages of a rain event, the enhanced model performs better in estimating high-temporal-resolution pollution loads. Also, pollution concentrations of rain events vary in a large range, leading to the need to average monitoring values of multiple rain events when using EMC method. This not only increases the workload but also loses the unique characteristics of each rainfall. In contrast, the enhanced model simulates pollution concentration based on physical processes, which enables stable and accurate characterization of runoff pollution.

## 4.2 Implications for non-point source pollution management

The first flush is considered to be key for controlling rainfall-runoff pollution because of its short duration and heavy pollution load[41]. In contrast to established models, our simulation (Fig. 7) shows that 12% of total runoff contains 80% to 95% of total pollution load for COD, TN and TP, which are dominated by land pollution (Group A). However, it only contains 15% of total pollution load for $NH_4^+$-N, which is dominated by wet precipitation (Group B). This means two strategies are necessary to mitigate rainfall pollution. For Group A, it is crucial to collect and treat runoff during the first 15 min to prevent pollution from entering drains or water courses. First flush diverters are commonly used in urban areas to collect runoff for treatment systems[42]. However, rainfall treatment facilities are uncommon in rural areas. Artificial wetlands, decentralized sewage treatment facilities and ecological ponds are recommended to accept the first flush from the drainage. Given the operating cost, accurately estimating duration and pollution load of first flush is required to reduce the treatment capacity of these systems[43], especially in rural areas with lower GDP. For Group B, the cumulative pollution load is proportional to time duration; therefore it is necessary to continuously collect all rainfall. Generally, the following steps are suggested for designing collection and treatment system of first flush: (1) identify the target pollutant, (2) determine if it is Groups A or B using the enhanced wash-off model, and (3) simulate the duration and pollution load of first flush or whole runoff. Also, direct removal of pollution in first flush and measures to reduce $m_0$ and k can be applied. Precision fertilization[44] can decrease nutrient surplus in agricultural lands, and waste management[45] can reduce the initial pollution load. The physical and chemical form of pollutants also needs to be considered because this influences wash-off potential. The relationships between k and factors including such as slope, land use and vegetation require investigation.

## 4.3 Model extrapolation and uncertainties

The enhanced model was developed based on physical processes including buildup, wash-off and wet precipitation, and theoretically can be applied in any region and to any pollutant. While earlier studies used the models mainly on impervious surfaces, this study proved that the enhanced model performs well in permeable lands such as the vegetable field. However, the model could also be used and validated in more land-use types such as village roads, roofs, waste dumping plots and courtyards. In future work, inhomogeneous rain intensity could be included in the model, and key factors influencing $m_0$ and k should be investigated.

Despite the clear improvement in the performance the enhance model, uncertainties persist due to several factors including limited observations of rainfall events and inadequate representation of diverse seasons, land-use types, slopes and rainfall amounts. Also, the assumption of constant rainfall intensity and rain pollution concentration made in this study is a simplification of real-world conditions. Consequently, the subsequent enhancement of the model should focus on incorporating non-uniform rainfall patterns into the model equations. In future work, precise observation of rainfall can be considered to address this issue. Additionally, the current model simulated the rainfall-runoff pollution for a single land

plot without considering the interactions among multiple plots. Addressing this limitation should significantly augment the utility of the model for estimating pollution loads associated with rainfall-runoff processes.

## 5 CONCLUSIONS

To improve the modeling of rainfall-runoff pollution, this study enhanced the wash-off model by introducing wet precipitation, and the relationship between rainfall and runoff. This enhanced wash-off model was validated in a typical rural-residential area in Gusheng Village in the Erhai Lake Basin. Our findings suggest the enhanced model is more effective because of the inclusion of pollutant concentration in wet precipitation thereby identifying two different categories of pollution: one dominated by land pollution and the other by rainfall pollution. Compared to the EMC method, the enhanced model more accurately simulated pollutant concentrations in runoff at high-temporal-resolution. The results show that 12% of the total runoff contains 80% to 95% of total load for COD, TN and TP whereas it contains only 15% of total load for $NH_4^+$-N. Based on more refined depiction of pollution load and temporal variation in rainfall, the enhanced model provides deeper insights into non-point pollution management especially the potential benefit of controlling the first flush.

**Acknowledgements**

This work was financially supported by the Key Science and Technology Program of Yunnan Province (202202AE090034), the Key Research and Development Program of Yunnan Province (202203AC100002), and the Erhai Academy of Green Development (EAGD).

**Compliance with ethics guidelines**

Mingjin Cheng, Xin Liu, Han Xiao, Fang Wang, Minghao Pan, Zengwei Yuan, and Hu Sheng declare that they have no conflicts of interest or financial conflicts to disclose. This article does not contain any studies with human or animal subjects performed by any of the authors.

## REFERENCES

1. Yu C, Huang X, Chen H, Godfray H C J, Wright J S, Hall J W, Gong P, Ni S, Qiao S, Huang G, Xiao Y, Zhang J, Feng Z, Ju X, Ciais P, Stenseth N C, Hessen D O, Sun Z, Yu L, Cai W, Fu H, Huang X, Zhang C, Liu H, Taylor J. Managing nitrogen to restore water quality in China. *Nature*, 2019, **567**(7749): 516–520
2. Chen X, Strokal M, Van Vliet M T H, Stuiver J, Wang M, Bai Z, Ma L, Kroeze C. Multi-scale modeling of nutrient pollution in the rivers of China. *Environmental Science & Technology*, 2019, **53**(16): 9614–9625
3. Xu H, Zhang Y, Zhu X, Zheng M. Effects of rainfall-runoff pollution on eutrophication in coastal zone: a case study in Shenzhen Bay, southern China. *Nordic Hydrology*, 2019, **50**(4): 1062–1075
4. Schaffner M, Bader H P, Scheidegger R. Modeling the contribution of point sources and non-point sources to Thachin River water pollution. *Science of the Total Environment*, 2009, **407**(17): 4902–4915
5. Lang M, Li P, Yan X. Runoff concentration and load of nitrogen and phosphorus from a residential area in an intensive agricultural watershed. *Science of the Total Environment*, 2013, **458–460**: 238–245
6. Ongley E D, Zhang X, Yu T. Current status of agricultural and rural non-point source pollution assessment in China. *Environmental Pollution*, 2010, **158**(5): 1159–1168
7. Yuan Z, Pang Y, Gao J, Liu X, Sheng H, Zhuang Y. Improving quantification of rainfall runoff pollutant loads with consideration of path curb and field ridge. *Resources. Environment and Sustainability*, 2021, **6**: 100042
8. Guo J, Pan Y, Zuo P, Xu Y, Wang Q, Ma J, Wang L. Accumulation and wash-off characteristics of surface pollutant and identification of risk areas on urban land uses in a lakeside city, Wuxi, China. *Urban Water Journal*, 2019, **16**(5): 323–333
9. Taebi A, Droste R L. First flush pollution load of urban stormwater runoff. *Journal of Environmental Engineering and Science*, 2004, **3**(4): 301–309
10. Wang S, He Q, Ai H, Wang Z, Zhang Q. Pollutant concentrations and pollution loads in stormwater runoff from different land uses in Chongqing. *Journal of Environmental Sciences*, 2013, **25**(3): 502–510
11. Charbeneau R J, Barrett M E. Evaluation of methods for estimating stormwater pollutant loads. *Water Environment Research*, 1998, **70**(7): 1295–1302
12. Zeng J, Huang G, Luo H, Mai Y, Wu H. First flush of non-

point source pollution and hydrological effects of LID in a Guangzhou community. *Scientific Reports*, 2019, **9**(1): 13865
13. Sartor J D, Boyd G B. Water pollution aspects of street surface contaminants. USA: *US Government Printing Office*, 1972, 2
14. Morgan D, Johnston P, Osei K, Gill L. A modified wash-off function for stormwater suspended solids modelling. *Journal of Hydrology*, 2020, **584**: 124672
15. Chaudhary S, Chua L H C, Kansal A. Modeling washoff in temperate and tropical urban catchments. *Journal of Hydrology*, 2021, **603**(Part B): 126951
16. Gaut J, Chua L H C, Irvine K N, Le S H. Modelling the washoff of pollutants in various forms from an urban catchment. *Journal of Environmental Management*, 2019, **246**: 374–383
17. Muthusamy M, Tait S, Schellart A, Beg M N A, Carvalho R F, de Lima J L M P. Improving understanding of the underlying physical process of sediment wash-off from urban road surfaces. *Journal of Hydrology*, 2018, **557**: 426–433
18. Soonthornnonda P, Christensen E R, Liu Y, Li J. A washoff model for stormwater pollutants. *Science of the Total Environment*, 2008, **402**(2–3): 248–256
19. Muthusamy M, Wani O, Schellart A, Tait S. Accounting for variation in rainfall intensity and surface slope in wash-off model calibration and prediction within the Bayesian framework. *Water Research*, 2018, **143**: 561–569
20. Ma M, Zheng B, Xu W, Cao J, Zhou K, Zhao Y. Trend and interannual variations of reactive nitrogen deposition in China during 2008–2017 and the roles of anthropogenic emissions and meteorological conditions. *Journal of Geophysical Research—Atmospheres*, 2023, **128**(6): e2022JD037489
21. Chou C M. Applying multiscale entropy to the complexity analysis of rainfall-runoff relationships. *Entropy*, 2012, **14**(5): 945–957
22. Lian H, Yen H, Huang J C, Feng Q, Qin L, Bashir M A, Wu S, Zhu A X, Luo J, Di H, Lei Q, Liu H. CN-China: revised runoff curve number by using rainfall-runoff events data in China. *Water Research*, 2020, **177**: 115767
23. Jia Z, Chang X, Duan T, Wang X, Wei T, Li Y. Water quality responses to rainfall and surrounding land uses in urban lakes. *Journal of Environmental Management*, 2021, **298**: 113514
24. Zhang Y, Yang Z, Liu J, Zhang X, Zhu G. Characteristics of rainfall runoff pollution and ecological purification efficiency in rural courtyards. *Water Purification Technology*, 2022, **41**(11): 113–120 (in Chinese)
25. Ministry of Ecology and Environment of the People's Republic of China. Environmental quality standards for surface water (GB 3838–2002). *Ministry of Ecology and Environment of the People's Republic of China*, 2002 (in Chinese)
26. Zhang S, Hou X, Wu C, Zhang C. Impacts of climate and planting structure changes on watershed runoff and nitrogen and phosphorus loss. *Science of the Total Environment*, 2020, **706**: 134489
27. Shaw S B, Walter M T, Steenhuis T S. A physical model of particulate wash-off from rough impervious surfaces. *Journal of Hydrology*, 2006, **327**(3–4): 618–626
28. Kim L H, Kayhanian M, Zoh K D, Stenstrom M K. Modeling of highway stormwater runoff. *Science of the Total Environment*, 2005, **348**(1–3): 1–18
29. Naves J, Rieckermann J, Cea L, Puertas J, Anta J. Global and local sensitivity analysis to improve the understanding of physically-based urban wash-off models from high-resolution laboratory experiments. *Science of the Total Environment*, 2020, **709**: 136152
30. Bonhomme C, Petrucci G. Should we trust build-up/wash-off water quality models at the scale of urban catchments? *Water Research*, 2017, **108**: 422–431
31. Hong Y, Bonhomme C, Le M H, Chebbo G. A new approach of monitoring and physically-based modelling to investigate urban wash-off process on a road catchment near Paris. *Water Research*, 2016, **102**: 96–108
32. Yuan Z, Jiang S, Sheng H, Liu X, Hua H, Liu X, Zhang Y. Human perturbation of the global phosphorus cycle: changes and consequences. *Environmental Science & Technology*, 2018, **52**(5): 2438–2450
33. Liu X, Sheng H, Jiang S, Yuan Z, Zhang C, Elser J J. Intensification of phosphorus cycling in China since the 1600s. *Proceedings of the National Academy of Sciences of the United States of America*, 2016, **113**(10): 2609–2614
34. Zou T, Zhang X, Davidson E A. Global trends of cropland phosphorus use and sustainability challenges. *Nature*, 2022, **611**(7934): 81–87
35. Jin X, Bai Z, Oenema O, Winiwarter W, Velthof G, Chen X, Ma L. Spatial planning needed to drastically reduce nitrogen and phosphorus surpluses in China's agriculture. *Environmental Science & Technology*, 2020, **54**(19): 11894–11904
36. Ma L, Wang F, Zhang W, Ma W, Velthof G, Qin W, Oenema O, Zhang F. Environmental assessment of management options for nutrient flows in the food chain in China. *Environmental Science & Technology*, 2013, **47**(13): 7260–7268
37. Cheng M, Quan J, Yin J, Liu X, Yuan Z, Ma L. High-resolution maps of intensive and extensive livestock production in China. *Resources, Environment and Sustainability*, 2023, **12**: 100104
38. Fritz S, See L, McCallum I, You L, Bun A, Moltchanova E, Duerauer M, Albrecht F, Schill C, Perger C, Havlik P, Mosnier A, Thornton P, Wood-Sichra U, Herrero M, Becker-Reshef I, Justice C, Hansen M, Gong P, Aziz S A, Cipriani A, Cumani R, Cecchi G, Conchedda G, Ferreira S, Gomez A, Haffani M, Kayitakire F, Malanding J, Mueller R, Newby T, Nonguierma A, Olusegun A, Ortner S, Rajak D R, Rocha J, Schepaschenko D, Schepaschenko M, Terekhov A, Tiangwa A, Vancutsem C, Vintrou E, Wu W, van der Velde M, Dunwoody A, Kraxner F, Obersteiner M. Mapping global cropland and field size. *Global Change Biology*, 2015, **21**(5): 1980–1992
39. Gao J, O'Neill B C. Mapping global urban land for the 21st century with data-driven simulations and shared socioeconomic pathways. *Nature Communications*, 2020, **11**(1): 2302
40. Batista E, Silva F, Freire S, Schiavina M, Rosina K, Marín-

Herrera M A, Ziemba L, Craglia M, Koomen E, Lavalle C. Uncovering temporal changes in Europe's population density patterns using a data fusion approach. *Nature Communications*, 2020, **11**(1): 4631

41. Perera T, McGree J, Egodawatta P, Jinadasa K B S N, Goonetilleke A. New conceptualisation of first flush phenomena in urban catchments. *Journal of Environmental Management*, 2021, **281**: 111820
42. Wang S, Feng L, Min F. Optimizing first flush diverter for urban stormwater pollution load reduction by most efficiently utilizing first flush phenomena. *Journal of Environmental Management*, 2023, **335**: 117563
43. Kang J H, Kayhanian M, Stenstrom M K. Implications of a kinematic wave model for first flush treatment design. *Water Research*, 2006, **40**(20): 3820–3830
44. Miao Y, Stewart B A, Zhang F. Long-term experiments for sustainable nutrient management in China. A review. *Agronomy for Sustainable Development*, 2011, **31**(2): 397–414
45. Liu X, Zhang Y, Cheng M, Jiang S, Yuan Z. Recycling phosphorus from waste in China: recycling methods and their environmental and resource consequences. *Resources, Conservation and Recycling*, 2023, **188**: 106669